

## ULTRASONIC NDE OF COMPOSITE PANELS WITH GAS-COUPLED LASER ACOUSTIC DETECTION

James N. Caron, and James B. Mehl  
Department of Physics  
University of Delaware  
Newark, DE 19716-2570

Karl V. Steiner  
Center for Composite Materials  
University of Delaware  
Newark DE 19716-3144

### INTRODUCTION

High resolution beam-deflection techniques have been applied to the ultrasonic inspection of materials. The technique is similar to air-coupled detection, with the airborne wave detected through beam deflection instead of with an electro-acoustic transducer. It is a non-contact, laser based, detection technique that does not require reflection of the detection laser beam from the surface. It is thus independent of the surface optical properties of the material under test.

The detection principle is the bending of an optical probe beam passing through a density gradient in a gas. The associated gradient in the optical index of refraction  $n(\mathbf{r})$  causes beam deflection, as described by the eikonal equation [1]. Optical beam deflection techniques have been extensively applied to the observation of thermal waves in gases [2–5]. Similar deflections from acoustic waves in gases are more difficult to detect because of the generally weaker spatial dependence of the gas density [6–8].

Sufficient sensitivity for application of the beam deflection technique to the ultrasonic inspection of materials has been obtained by use of a 532 nm cw diode-pumped laser and a custom-built position-sensitive photodetector. Gas-coupled laser acoustic detection (GCLAD) has been used to detect ultrasonic waveforms in a variety of materials, and as the detection element in ultrasonic C-scans of various polymer/graphite composite panels.

The basic experimental arrangement is shown in Figure 1. Ultrasonic waveforms, generated by a pulsed laser or contact transducer at the upper surface of the sample, propagate within the sample and are repeatedly reflected from the lower and upper surfaces. During each reflection, a fraction of the ultrasonic power is radiated as an airborne wave. This acoustic wave has density and optical index of

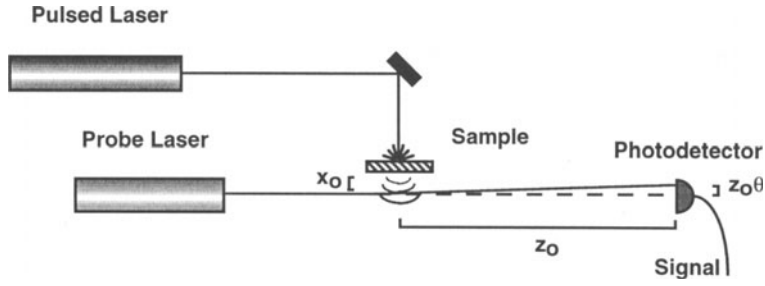


Figure 1. Experimental arrangement for observation of laser-generated ultrasonic waveforms with GCLAD. Ultrasonic waves propagate through the sample and, upon incidence at the lower surface, radiate an airborne wave which causes deflection of an optical probe beam.

refraction gradients perpendicular to the surface of the sample. The probe beam, directed parallel to the surface of the sample, is deflected when it passes through a region with a transverse gradient in the index of refraction. The beam deflection is measured with a position-sensitive photodetector.

In contrast to interferometric detection, GCLAD does not require reflecting or scattering an optical beam from the sample surface. It is thus independent of the surface optical properties of the sample. It can be applied to a large class of materials. Samples can be interchanged without extensive optical adjustments. The sensitivity with untreated samples is comparable or greater to that obtained with painted samples when using our confocal Fabry-Perot-based detection system [9], which uses a 200 mW detection laser. The GCLAD system is comparatively simple, and utilizes no specialized optics or stabilizing electronics. The frequency response is broad-band, with high frequency limits caused by the increasing attenuation of the acoustic wave at higher frequencies.

## THEORY

An expression for the beam deflection angle  $\theta$  which results from an acoustic density variation can be deduced from the eikonal equation

$$\frac{d}{ds} \left( n(\mathbf{r}) \frac{d\mathbf{R}(\mathbf{r})}{ds} \right) = \nabla n(\mathbf{r}). \quad (1)$$

Here  $\mathbf{R}(\mathbf{r})$  is the path of a light ray and  $ds$  is the element of path length along the ray. An acoustic wave radiated from the lower surface of the sample in Figure 1 will be assumed to be approximately a plane wave over the region of interaction with the probe beam, with the acoustic pressure having the form  $p(x + ut)$ , where  $u$  is the speed of sound. The acoustic density is  $p/u^2$  [10]. The index of refraction can be calculated from

$$n^2 - 1 \approx 3A\rho/M, \quad (2)$$

where  $A$  is the molar refractivity [1] and  $M$  is the molar mass. In an acoustic wave the index of refraction will be  $n_0 + n_a$ , with

$$n_a \approx \frac{3A}{2n_0} \frac{p}{Mu^2} = (n_0 - 1) \frac{p}{\rho u^2}. \quad (3)$$

In the weak-deflection limit,  $s \approx z$  and the  $x$ -component of Equation (1) is approximately

$$\frac{d^2 X(z)}{dz^2} = \frac{1}{n_0} \frac{\partial n_a(x)}{\partial x}. \quad (4)$$

The angle of deflection, assumed small, is

$$\theta = \tan^{-1} \left( \frac{dX}{dz} \right) \approx \frac{dX}{dz}. \quad (5)$$

The left side of Equation (4) is thus  $d\theta/dz$ , and the gradient of  $n_a$  on the right side can be expressed as either a spatial or temporal derivative of the acoustic pressure

$$\frac{d\theta}{dz} = \frac{n_0 - 1}{\rho u^2} \frac{\partial p}{\partial x} = \frac{n_0 - 1}{\rho u^3} \frac{\partial p}{\partial t}. \quad (6)$$

The total deflection of the beam is thus

$$\theta \approx \frac{n_0 - 1}{\rho u^3} \int \frac{\partial p}{\partial t} dz. \quad (7)$$

For air under ambient conditions, the index of refraction at 532 nm is 1.0002939 [1]. Also for ambient air, the quantity  $\rho u^2$  is approximately  $1.4p_0$ , where  $p_0$  is the ambient pressure  $\approx 10^5$  Pa. The derivative  $\partial p/\partial t$  is of order  $2\pi f p$  for an acoustic wave of frequency  $f = u/\lambda$ , where  $\lambda$  is the wavelength. The total beam deflection is thus approximately

$$\theta \approx 1.3 \times 10^{-3} \frac{p}{p_0} \frac{\Delta z}{\lambda}, \quad (8)$$

where  $\Delta z$  is the width of the intersection of the acoustic and probe beams.

## ACOUSTIC WAVE RADIATED BY A TRANSDUCER

Figure 2 shows a stationary optical beam incident upon a photodetector mounted on a translation stage. The detector output as a function of position was measured and used for calibration of the system. The system was tested by directing the probe beam parallel to a 1 MHz piezoelectric transducer. The beam deflection observed on the photodetector, located  $z_0 = 2$  m from the transducer, is shown in

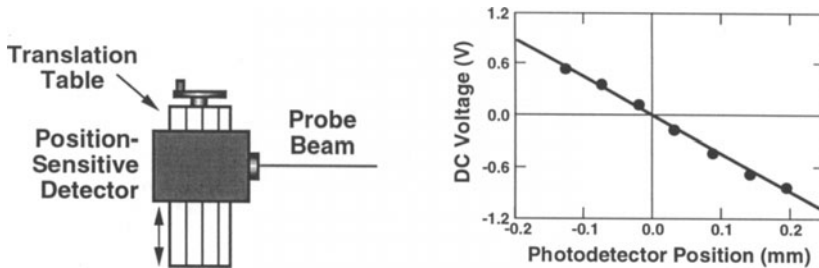


Figure 2. Calibration setup and data for photodetector as a function of transverse position. The scatter in the plot of photodetector output vs. position is due to limited resolution of the translation measurement. The slope of a line fit through the points is used for calibrating the beam deflection measurements in angular units.

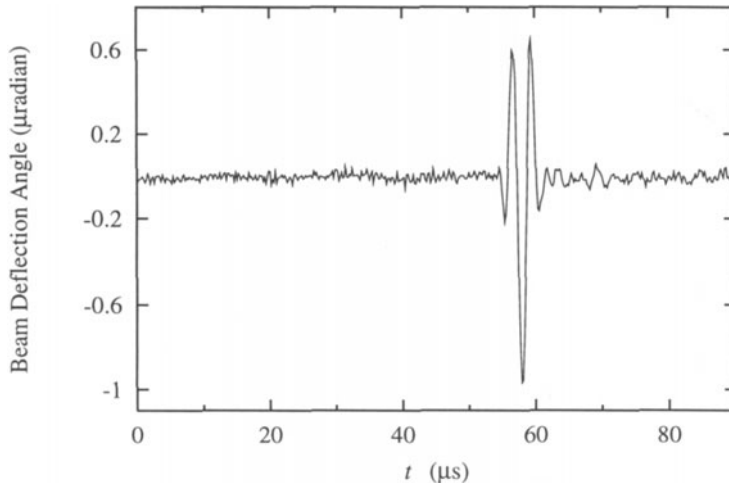


Figure 3. An acoustic waveform radiated directly into air from a 1 MHz transducer, measured with the GCLAD photodetector 2 m from the transducer.

Figure 3. This waveform represents a single scan without averaging. The maximum negative signal ( $-1 \mu\text{radian}$ ) corresponds, according to Equation (8), to an acoustic pressure of order 2 Pa. The noise level away from the peak is of order 0.04 Pa.

The frequency response of the detection electronics used in these measurements has not yet been characterized. However, it is clear that the system is sufficiently fast for observation of ultrasound at frequencies near 1 MHz.

## LASER-GENERATED WAVEFORMS

GCLAD provides an alternative detection technique for laser-based ultrasonic inspection of materials [11,12]. It is similar to detection with air-coupled transducers [13,14], but does not have the bandwidth limitations of air-coupled transducers.

As noted above, GCLAD is independent of the surface optical properties of the material under test. Different samples can be rapidly interchanged. Waveform measurements in several samples taken with the system shown in Figure 1 are displayed in Figure 4. Ultrasound was generated by a pulsed 1064 nm Nd:YAG laser incident on the upper surface of the sample in Figure 1. The ultrasonic signals echo several times within the sample, and radiate an acoustic wave at each reflection. The beam deflections resulting from the acoustic waves were observed on a photodetector located 1 m from the samples.

The displayed waveforms were generated in a 16-layer AS-4/PEEK pultruded rod, a 16-layer AS-4/PEEK composite panel, and an 8-layer AS-4/PEKK tow-placed panel. The generating spot size was  $0.2 \text{ cm}^2$ . The waveforms were generated in the thermoelastic regime. The detected waveforms were digitally averaged over 25 shots. The distance  $x_0$  from sample to the probe beam was about 5 mm. The differences in

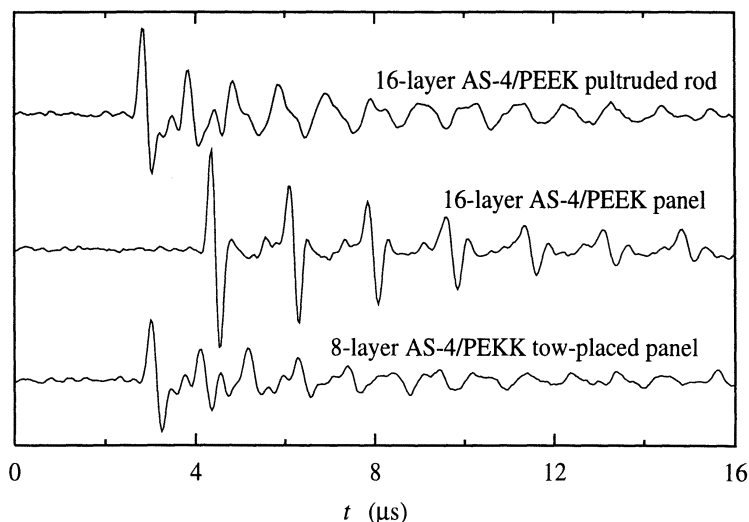


Figure 4. Laser generated/GCLAD detected ultrasonic waveforms in various graphite/polymer composites. The laser pulse strikes the sample at  $t = 0$ . The time to the first wave is a combination of the time-of-flight in the solid, and the time-of-flight in the air gap between the sample and the probe beam.

the time to the first longitudinal waves are attributed to small variations in this distance. The graph shows many longitudinal wave echoes, the transverse wave, and mode conversion of the transverse wave into longitudinal waves.

Waveforms have also been detected in various metals and polymer materials. However, graphite/polymer composites present particular difficulties for laser-based interferometric techniques. These composites typically have optically rough surfaces and high optical absorption, so that only weakly reflected light is available for interferometry. These problems are inconsequential for GCLAD.

#### LASER-BASED ULTRASONIC INSPECTION

Through-transmission C-scans (planar ultrasonic images) of composite samples were generated using GCLAD in the configuration of Figure 5. Two computer-controlled, screw-driven arms translated the sample perpendicular to the generation beam and parallel to the probe beam. The range of the scans was set to  $50 \times 50 \text{ mm}^2$  with a resolution of  $1 \text{ mm}^2/\text{pixel}$  for these preliminary experiments. The pulsed laser energy was set so that generation took place below the ablation threshold for each sample. The detection beam was positioned about 4 mm from the sample, and followed a 2 m path, folded with mirrors, to the photodetector. Each pixel represents the average of the amplitudes of six laser-generated waveforms.

Figure 6 shows C-scans of 16- and 32-layer AS-4/epoxy composite panels which had been subjected to impact testing. Lighter pixels represent better acoustic energy transmission. Darker areas indicate delaminations. The subsurface flaws are clearly resolved.

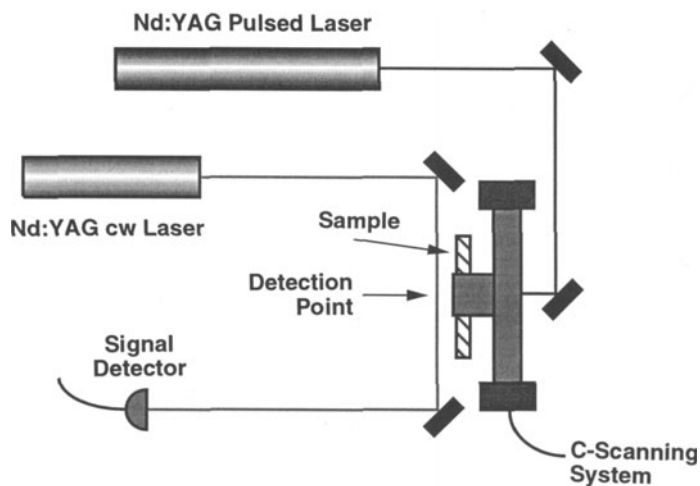


Figure 5. Ultrasonic C-scan system using pulsed-laser generation and GCLAD detection of the acoustic waveforms.

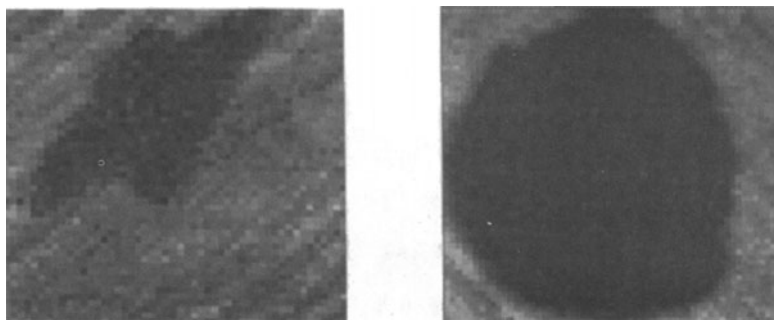


Figure 6. 50×50 mm<sup>2</sup> laser-generated/GCLAD detected C-scans of 16-layer (left) and 32-layer (right) AS-4/epoxy composite panels with subsurface impact damage.

Figure 7 shows two C-scans of an 8-layer AS-4/PEKK tow-placed composite panel. The left scan was made with GCLAD; the right scan was made with our confocal Fabry-Perot (CFP) interferometer-based detection system [9]. Frequency drift in the laser caused occasional loss of synchronization with the CFP, observable as dark pixels in the right image. In contrast, the GCLAD C-scan shows no loss of signal and better resolution. In addition, a reflective coating applied to the sample surface was necessary to conduct the inspection using the CFP-based system. Coating was not required for the GCLAD-scan.

Figure 8 shows C-scans of a 32-layer AS-4/PEEK composite panel which had been subjected to impact testing, as detected by GCLAD and a by a conventional 15 MHz focused transducer in an immersion tank. The subsurface flaws are clearly resolved in both scans. Variations resulting from the lay-up of the graphite fibers can also be seen.

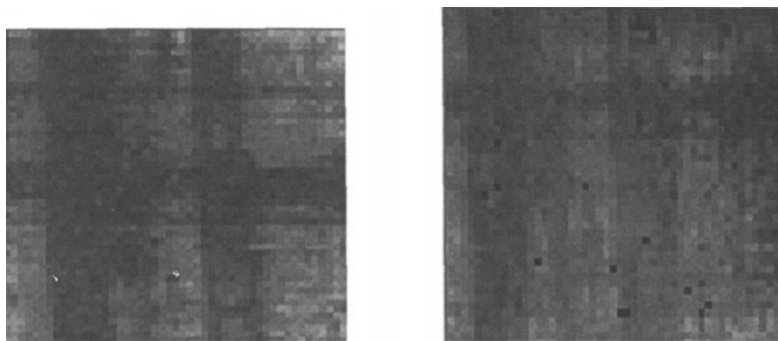


Figure 7. 50×50 mm<sup>2</sup> laser-generated C-scans of an 8-layer AS-4/PEKK composite panel with tow-placed flaws as detected by GCLAD (left) and a confocal Fabry-Perot interferometer-based detection system (right). (There is a 20 mm vertical displacement between the two scans.)

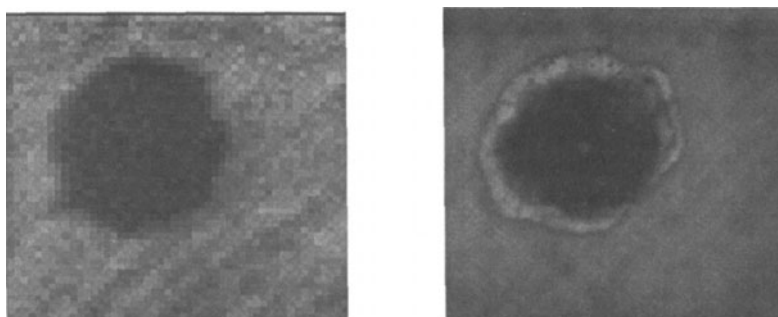


Figure 8. 50×50 mm<sup>2</sup> ultrasonic C-scans of a 32-layer AS-4/PEEK composite panel with subsurface impact damage as detected by GCLAD (left) and a 15 MHz focused transducer in an immersion tank (right).

## CONCLUSIONS

Gas-coupled laser acoustic detection has been applied to ultrasonic inspection of materials. Laser-generated waveforms have been detected in a variety of materials and ultrasonic C-scans have been performed on various graphite/polymer composite panels. The sensitivity of the detection technique is comparable with laser-based interferometric techniques with low-power detection lasers and painted samples, but is totally independent of the optical properties of the material surface such as reflectivity and optical smoothness. The system also requires no specialized optics or stabilization circuitry. Like air-coupled transducers, system response is dependent on the attenuation properties of the gas medium, but does not have the bandwidth limitations of air-coupled transducers.

In future work the frequency response of GCLAD will be systematically investigated, and the limits of resolution of C-scans with GCLAD will be determined. Preliminary experiments have already shown that GCLAD can be used for single-surface measurements of surface acoustic waves.

## ACKNOWLEDGEMENT

The authors gratefully acknowledge the support of this work through the Army Research Office/University Research Initiative grant, "Multidisciplinary Program in Manufacturing Science of Polymeric Composites."

## REFERENCES

1. M. Born and E. Wolf, *Principles of Optics*, (Pergamon Press: London, 1959).
2. J.C. Murphy and L.C. Aamodt, *J. Appl. Phys.* 51, 4580 (1981).
3. G.C. Wetsel, Jr. and S.A. Stotts, *Appl. Phys. Lett.* 42, 932 (1983).
4. A. C. Tam, *Rev. Mod. Phys.* 58, 381 (1986).
5. A. Mandelis (ed.), *Principles and Perspectives of Photothermal and Photoacoustic Phenomena*, (Elsevier, New York, 1992).
6. J.A. Sell, D.M. Heffelfinger, P.L.G. Ventzek, and R. M. Gilgenbach, *J. Appl. Phys.* 69, 1330 (1991).
7. J. Diaci, *Rev. Sci. Instr.* 63, 5306 (1992).
8. J. Diaci and J. Možina, *Rev. Sci. Instr.* 66, 4644 (1995).
9. J.N. Caron, Y. Yang, J.B. Mehl, and K.V. Steiner, in *Review of Progress in Quantitative Nondestructive Evaluation*, Vol. 16, eds. D.O. Thompson and D.E. Chimenti (Plenum, New York, 1996).
10. P. M. Morse and K. U. Ingard, *Theoretical Acoustics*, (McGraw-Hill: New York, 1968).
11. C.B. Scruby and L.E. Drain, *Laser Ultrasonics*, (Adam Hilger: Bristol, 1990).
12. J.W. Wagner, in *Physical Acoustics*, Vol. 19, R.N. Thurston and A.D. Pierce, eds., (Academic, New York, 1990).
13. D.A. Hutchins, W.M.D. Wright, and G. Hayward, *IEEE Trans. Ultrason. Ferroelectr. Freq. Control* 41, 796 (1994).
14. W.M.D. Wright, D.W. Schindel, and D.A. Hutchins, *J. Acoust. Soc. Am.* 95, 2567 (1994).